Seismic Performance of Pile-Supported Piers and Wharves Subjected to Foundation Deformations

Milad Souri[1]; Arash Khosravifar, Ph.D., P.E., M.ASCE[2];
Stephen Dickenson, Ph.D., P.E., D.PE, M.ASCE[3]; Scott Schlechter, P.E., G.E., M.ASCE[4];
and Nason McCullough, Ph.D., P.E., G.E., M.ASCE[5]

[1]Dept. of Civil and Environmental Engineering, Portland State Univ., Portland, OR 97201. E-mail: msouri@pdx.edu
[2]Dept. of Civil and Environmental Engineering, Portland State Univ., Portland, OR 97201. E-mail: karash@pdx.edu
[3]New Albion Geotechnical, Inc., Reno, NV 89509. E-mail: sed@newalbiongeotechnical.com
[4]GRI, Beaverton, OR 97008. E-mail: SSchlechter@gri.com
[5]Jacobs, Corvallis, OR 97330. E-mail: Nason.McCullough@jacobs.com

ABSTRACT

The interaction of inertial and kinematic demands is investigated using data from five physical models of pile-supported wharves using a large-scale geotechnical centrifuge. The wharf structures in this study were subjected to a suite of recorded ground motions, therefore associated superstructure inertia, and earthquake-induced slope deformations of varying magnitudes. The observations from these tests were used to provide insights on how to estimate large bending moments that developed at pile head and at depths significantly below a commonly assumed point of fixity that are associated with deep-seated ground deformations. Design recommendations are proposed on how to combine inertial and kinematic demands in a manner that is representative of the global structure.

INTRODUCTION

Pile-supported wharves subjected to earthquake motions are designed to accommodate inertial loads imposed at pile head from the superstructure as well as the kinematic loads imposed on piles from the lateral ground deformations adjacent to the structure. The ground deformations are caused by shear strains in the weak, cyclically degradable foundation soils, the slope or embankment, and the backland areas.

ASCE 61-14 (Section 4.7) requires that simultaneous application of inertial and kinematic loads be considered taking into account the phasing and the locations where these loads are applied. The commentary of ASCE 61-14 (Section C4.7) suggests that these two loads (inertia and kinematics) are often considered to act at different times during the ground motion; therefore, they can be assumed uncoupled in design. This commentary mentions that this assumption should be checked on a project-specific basis. It also suggests that the inertial load tends to result in large bending moments at pile head while the kinematic loads tend to result in large bending moments at depth. The ASCE 61-14 (Section 4.7.2) specifically refers to the permanent portion of lateral ground deformations to be used to estimate the kinematic demands on piles. The commentary for this section describes different methods with various complexities to estimate the permanent lateral ground deformations, including the simplified Newmark sliding block analysis to more detailed two-dimensional dynamic soil-structure interaction analyses of the entire soil-structure system.

Other design codes provide varying recommendations on the combination of inertia and

kinematics. Pertinent examples include;

- ASCE 7-16 does not require combining lateral spreading and inertia;
- AASHTO (2014) recommends designing piles for simultaneous effects of inertia and lateral spreading only for large magnitude earthquakes (M>8);
- California and Oregon DOT's recommend 100% lateral spreading + 50% inertia (Caltrans 2012, ODOT 2014);
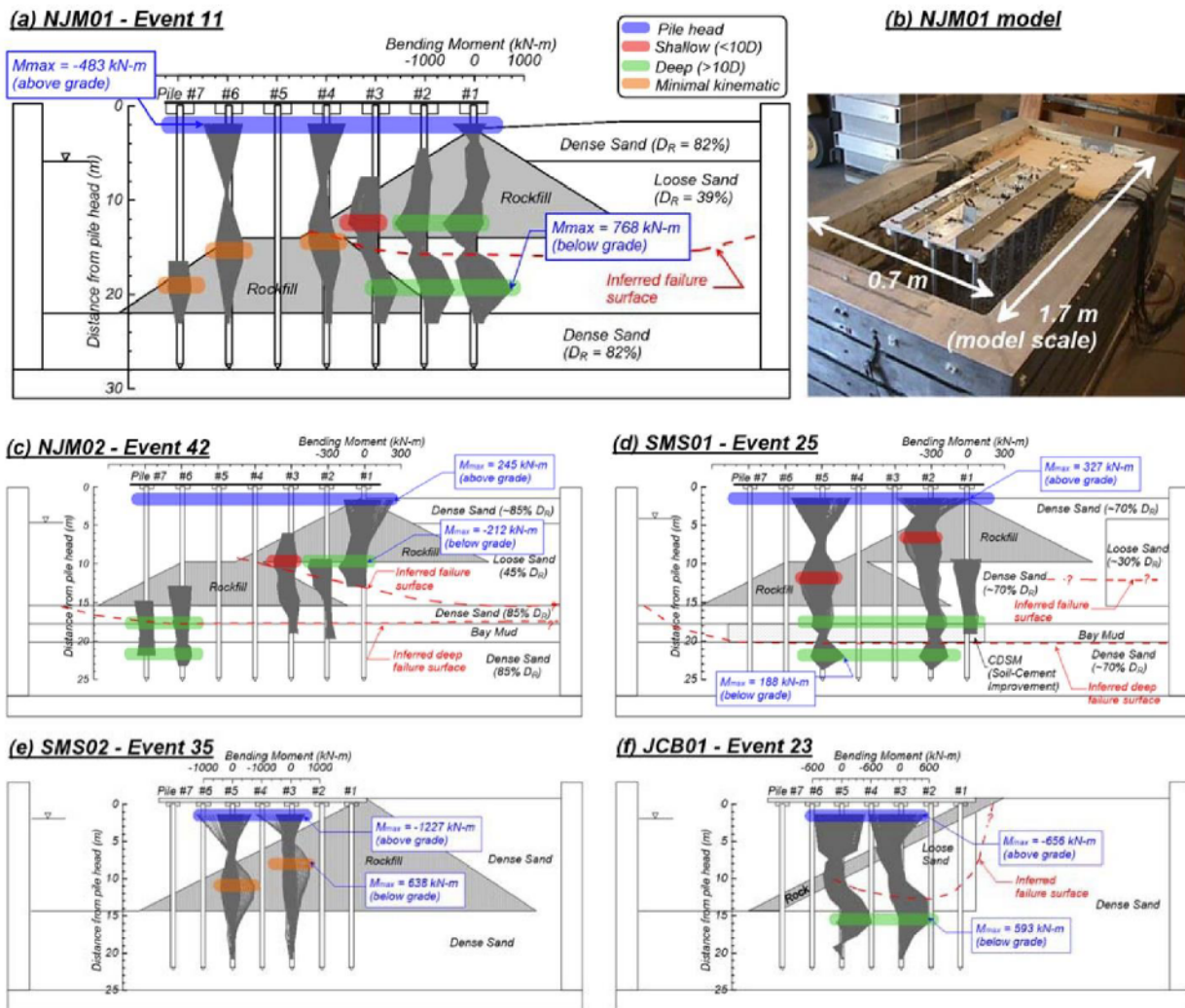- Washington DOT recommends 100% lateral spreading + 25% inertia (WSDOT, 2015).

Figure 1. Cross sections of five centrifuge tests along with envelopes of bending moment profiles, and inferred failure surfaces.

While numerical modeling is often used in design to develop bracketed load combination factors from synchronous timing of inertia and kinematics, we use physical modeling in this paper to evaluate the time-dependent interaction of inertia and kinematics noting that while the peak loads induced by these two conditions may not occur simultaneously there is always at least a portion of both loads acting on piles throughout the duration of the seismic loading. The physical modeling has been completed using the large-scale geotechnical centrifuge at UC Davis (McCullough et al. 2001). Centrifuge modeling is widely used to model soil-foundation-

structure- interaction (SFSI) for transportation systems, tunnels, and offshore structures (e.g., Dobry et al. 2003, Brandenberg et al. 2005, Chou et al. 2011, and Zhou et al. 2017). The centrifuge tests provide useful case-study simulations that are commonly used as the basis for calibrating simplified and complex numerical models that are used in practice (e.g. Travasarou et al. 2011).
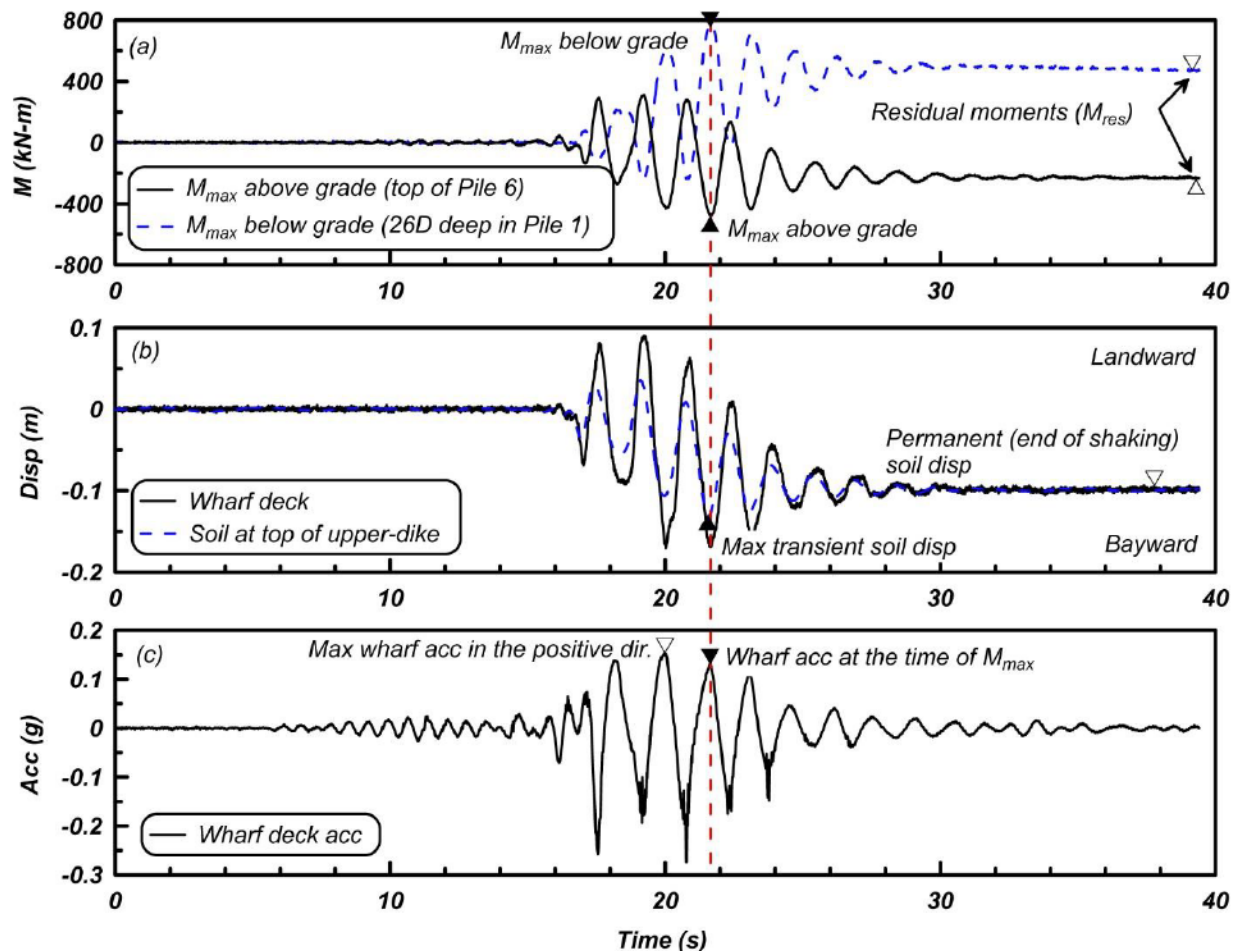

Figure 2. Representative time histories of (a) bending moments, (b) soil and wharf deck displacements, and (c) wharf deck inertia for the first major shaking in NJM01

The following section of this paper provides an overview of the five centrifuge tests that were used in this study. This section is followed by a summary of the analyzed data on the relative magnitude of inertial and kinematic demands at the time(s) when the peak bending moments are observed at the pile head and at depth. Implications for design are provided based on the results of pseudo-static analyses in *LPILE* to provide insights on when to combine inertial and kinematic loads in design to estimate peak bending moments in piles. Concluding remarks are provided based on the observations from these centrifuge tests.

EXPERIMENTAL STUDY

Centrifuge Tests: Table 1 lists the five tests analyzed in this study along with the key pile, superstructure, and soil properties and the applied ground motions. All tests included a wharf deck supported by 21 piles in a 7-by-3 setup. The piles were steel pipe piles with outer diameters

ranging from 0.38 m (1.25 ft) to 0.64 m (2 ft) (in prototype scale). Figure 1 shows the cross sections of the five centrifuge models. Figure 1a shows the cross section of the first centrifuge model (NJM01) and Figure 1b shows a photo of the model before shaking. The subsurface conditions in NJM01 included multi-lift rock dikes, a loose sand layer that liquefied during shaking and resulted in lateral spreading, a dense sand layer above the water table and a dense sand layer at pile tips. The inferred failure surface during cyclic loading was determined based on the soil displacement profiles and is shown with a red dashed line. The envelopes of maximum bending moment distributions during the ground motions are shown along the instrumented piles in gray. The locations where large bending moments were observed are color-coded according to the following categories: top of pile (blue), shallow locations with depth < 10D (red), deep locations with depth > 10D (green), and piles subjected to minimal kinematic demands (orange). The locations of maximum bending moments above and below grade are shown in this figure, which will be discussed later in the paper. It should be noted that while the envelopes of the maximum pile moments are useful for highlighting zones of importance, the plots do not demonstrate the time- dependent nature of the maximum moments as functions of depth or pile row (i.e., the peak moments are not experienced at the same time along a single pile or in all piles simultaneously).
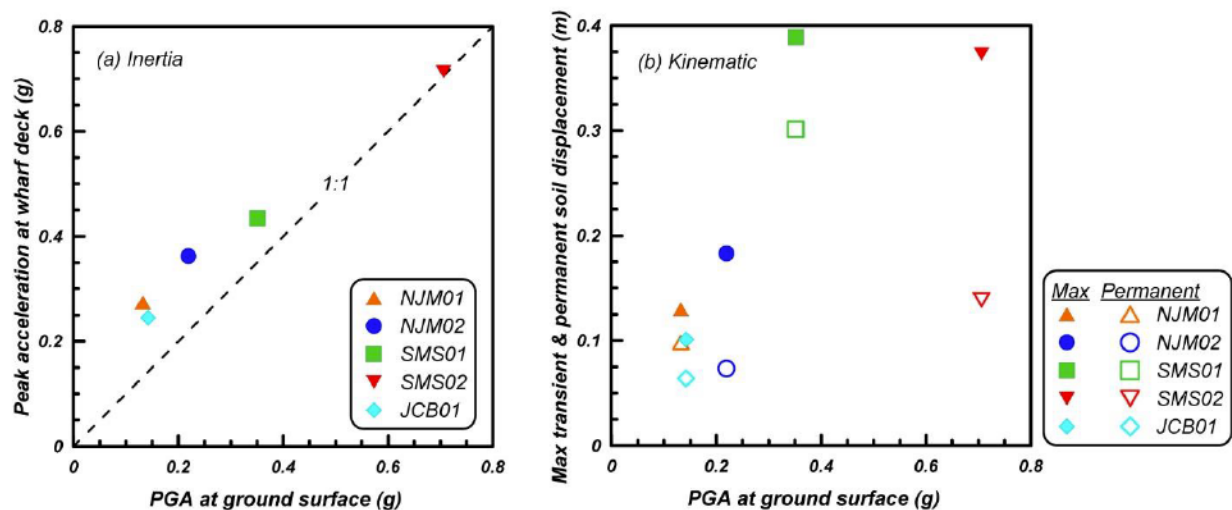

Figure 3. (a) Comparison of the peak acceleration at wharf deck (superstructure inertia) and peak acceleration at the ground surface (PGA), and (b) comparison of maximum transient and permanent soil displacements, and ground surface PGA

Figures 1c to 1f show the cross sections of the other four centrifuge models (NJM02, SMS01, SMS02 and JCB01) illustrating similar information as those in Figure 1a for NJM01. In NJM02 a relatively soft Bay Mud layer was included. In SMS01 a cement-deep-soil-mixing unit (CDSM) was incorporated. In SMS02 a single monolithic rock dike was supported by dense sand. In JCB01, the rock dikes were replaced with a thin layer of rock face.

In general, the observed zone of shear failure in the liquefied sand in the vicinity of piles can be characterized as broad, diffuse shear failure combined with a localized shear plane at the interface of weak and resistant layers such as the liquefied sand and the upper rockfill. Localized shear planes were also developed above Bay Mud in NJM02 and below CDSM in SMS01, which contributed to the large bending moments that developed at depth in those tests.

Table 1. Pile geometries, superstructure geometries, soil properties and ground motions in five centrifuge tests

Test ID [1]	Pile properties [2]	Superstructure properties	Soil properties	Applied ground motion at base	PGA at base (g)
NJM01	Pile D = 0.64 m, t = 0.036 m, L = 27.23 m, EI = 2.134e5 kPa-m4	Wharf deck 33.7 m × 15.2 m × 0.25 m, mass = 714774 kg	Nevada loose sand DR = 39 % Nevada dense sand, DR = 82 % Rockfill, friction angle =45 deg	Event 11. Loma Prieta 3	0.15
NJM02	Pile D = 0.38 m, t = 0.036 m, L = 25.063 m, EI = 4.113e4 kPa-m4	Wharf deck 24.9 m × 12.2 m × 0.25 m, mass = 265727 kg	Nevada loose sand DR = 45 % Nevada dense sand, DR = 85 % Bay Mud, undrained shear strength = 38 kPa Rockfill, friction angle = 45 deg	Event 42. Loma Prieta 3	0.19
SMS01	Pile D = 0.38 m, t = 0.036 m, L = 25.063 m, EI = 4.113e4 kPa-m4	Wharf deck 24.9 m × 12.2 m × 0.25 m, mass = 265727 kg	Nevada loose sand DR = 30 % Nevada dense sand, DR = 70 % CDSM, unconfined compressive strength = 0.9 MPa Rockfill, friction angle = 45 deg	Event 25. Loma Prieta 3	0.42
SMS02	Pile D = 0.64 m, t = 0.036 m, L = 24.26 m, EI = 2.134e5 kPa-m4	Wharf deck 28.1 m × 12.0 m × 0.78 m, mass = 951549 kg	Nevada dense sand, DR = 70 % Rockfill, friction angle = 45 deg	Event 35. Northridge 4	0.56
JCB01	Pile D = 0.64 m, t = 0.036 m, L = 24.26 m, EI = 2.134e5 kPa-m4	Wharf deck 28.1 m × 12.0 m × 0.78 m, mass = 951549 kg	Nevada loose sand DR = 40 % Nevada dense sand, DR = 74 % Rockfill, friction angle = 45 deg	Event 23. Loma Prieta 3	0.15

1. The centrifuge scale factor was 40.1 for all tests.
2. Pile group consists of 21 piles (in a 3-by-7 setup).
3. 1989 Loma Prieta Outer Harbor Station.
4. 1994 Northridge Rinaldi Station. This time history was recorded less than 10 km from the fault and included a velocity pulse.

The location of the shear planes explain how large bending moments developed below grade. It is significant that the large bending moments that were observed at depth (color-coded green) are below a typically assumed depth of fixity. The depth of fixity ranges from 5D to 7D for the piles studied here. The 10D depth that was used to distinguish deep bending moments (color-coded green) corresponds to z/T of 3 if depth (z) is normalized by the relative stiffness factor (T) (i.e., $T = (EI/k)^{(1/5)}$ where EI is the pile bending stiffness and k is the subgrade reaction in rockfill). The 10D depth is aligned with the definition of "deep in-ground" plastic hinge location per ASCE 61-14.

Representative Time Histories: Figure 2 provides representative time histories of pile moment, displacement, and wharf deck acceleration from test NJM01 to illustrate the time- and depth- dependent nature of the inertial and displacement demands on two piles (one which experienced the greatest inertial loading at the pile head and one that experienced the greatest kinematic loading at depth during shaking). Figure 2a shows the maximum transient bending moments below and above grade recorded in the test. The maximum moment above grade was recorded at the top of Pile 6 and the maximum moment below grade was recorded 17 m (56 ft) deep (26D) in Pile 1 above the interface between the loose liquefied sand and the underlying dense sand. These maximum transient moments both occurred at approximately the same time, as denoted with a vertical dashed line. The residual (end of shaking) moments are denoted in this figure showing that the residual bending moments were significantly smaller than the maximum transient bending moments.

Figure 2b shows the wharf deck and soil displacements. The maximum transient displacement and the permanent (end of shaking) displacements are also denoted in this figure suggesting that the maximum transient soil displacement (0.13 m or 5 in bayward) is approximately 1.3 times larger than the permanent soil displacement (0.1 m or 4 in bayward). This difference highlights the need for considering maximum transient soil displacements in design rather than the end of shaking, residual displacements. It is worthwhile noting that existing design methods (e.g., Newmark sliding block, and linear/nonlinear time-history analysis) provide an estimate of maximum transient and/or permanent soil displacements with various levels of conservatism.

Figure 2c shows the wharf acceleration, which is directly correlated with superstructure inertia. As plotted, positive wharf acceleration corresponds to bayward inertia. It is significant to note that in this model test the wharf inertia and the soil displacement were always in-phase. In addition, the peak moments at both the pile head and at depth were synchronous with the peak transient soil and wharf deck displacements. At this time the wharf acceleration was approximately 85% of its peak in the corresponding direction (i.e., the peak moment at the pile head did not occur at the time of peak inertial loading).

Range of Inertial and Kinematic Demands: Figure 3a shows the peak acceleration at wharf deck (superstructure) versus the peak ground acceleration (PGA) at ground surface for the five tests analyzed here. The wharf peak accelerations (indicative of the peak inertial demand) in this study range from 0.25g to 0.7g. The data supports a nonlinear relationship between the wharf deck peak acceleration and the ground surface PGA across the 5 tests evaluated.

Figure 3b shows the maximum transient and permanent (end of shaking) soil displacements measured by a Linear Variable Differential Transformers (LVDT) installed in the backland behind the wharf deck. The maximum transient soil displacements in the backland (indicative of the kinematic demands) range from 0.07 m to 0.4 m (2.8 to 15.7 in), and the permanent soil displacements range from 0.06 m to 0.3 m (2.4 to 11.8 in). It is observed from these tests that the

maximum transient soil displacements are 1.3 to 2.7 times larger than the permanent soil displacements. It is acknowledged that this ratio depends on soil properties, layering, and ground motion characteristics; however, it is noticed that in all five tests, this ratio was greater than one suggesting that the maximum transient soil displacements should be considered in design to estimate kinematic demands rather than the permanent (end of shaking) displacements. The soil displacements in SMS02 follow a noticeably different trend than other tests as the subsurface conditions in SMS02 included rockfill and dense sand that did not liquefy.

Location of Maximum Bending Moments: From a design perspective, it is important to estimate the location of maximum moments in the entire pile group and to determine whether the maximum moment occurs above the grade (e.g. at the pile head) or below the grade. The bending moments below grade can develop at the typical depth of fixity in cases with minimal kinematic demands or at large depths driven by significant soil deformations. The location and magnitude of maximum bending moments above and below grade were previously shown in the cross sections in Figure 1. Figure 4 shows a comparison of the magnitude of the maximum transient bending moments above and below grade observed in any pile within the group (i.e., the maximum moments were not necessarily experienced in the same pile). With the exception of NJM01, the bending moments above grade (at pile head) were equal to or larger than the maximum bending moments below grade. This ratio was approximately 1 for tests NJM02, SMS01, and JCB01, where liquefaction was triggered and significant kinematic demands were imposed. The ratio was approximately 1.9 in SMS02, where liquefaction was not triggered and kinematic demands were small. It should also be noted that maximum bending moments below grade in SMS02 were encountered at typical depth of fixity rather than at more significant depths in other tests with liquefiable soils.

COINCIDENCE OF INERTIAL AND KINEMATIC DEMANDS

Wharf Inertia at the Time of Maximum Bending Moments: Figure 5(a) shows a comparison of the normalized wharf acceleration (Acceleration at time = t / maximum wharf acceleration) at the time of maximum bending moment for locations above grade and below grade. The wharf accelerations at time t are normalized by the maximum wharf acceleration in the corresponding direction, i.e. positive accelerations are normalized by the maximum positive acceleration and negative accelerations are normalized by the maximum negative acceleration. This figure demonstrates that when pile head bending moments are at the maximum value, the wharf acceleration is, on average, at 92% of its peak (ranging between 84% to 100%). This relationship confirms, as expected, that peak moments at the pile-deck connection and near the pile head are synchronous with, and well-correlated with peak wharf deck acceleration. Conversely, peak moments at depth are not well-correlated with peak wharf deck PGA, as indicated by the significant variability in the normalized acceleration at the time of the peak moments at depth.

Maximum Transient and Residual Bending Moments: The physical model tests outlined in this paper indicate that the residual, end of shaking bending moments due to permanent soil displacement are smaller than the maximum moments that the piles experience during shaking. This is due, in part, to the fact that the peak transient pile moment reflects the synchronous application of inertial and kinematic effects, while the residual, post-shaking, pile moment is in response to only the permanent pile curvature demand related to the final soil displacement. The difference between the peak, transient and residual moments is a function of both the soil conditions and slope configuration, and the characteristics of the strong ground motions,

therefore the timing and extent of the seismically-induced slope deformation. Figure 5b shows the residual bending moments normalized by the maximum transient bending moments for two locations along a single pile (one above and one below grade). This figure shows that the residual moments are approximately 14% and 48% of their peak transient values for above grade and below grade locations, respectively. These ratios suggest that both the transient and residual moments should be evaluated in seismic design. This conclusion applies to relatively flexible piles, such as the ones studied here, where the piles follow the soil displacement patterns closely, reducing the relative displacement between soil and pile such that the ultimate soil reactions (i.e. the p_{ult} in p-y springs) do not mobilize. In these cases, the soil reaction, and therefore the bending moments, are proportional to soil displacements.

The kinematic demands on flexible piles can be best estimated by imposing the soil displacements to the end nodes of p-y springs, rather than imposing them as a lateral spreading pressure. This conclusion may not apply to the relatively stiff piles, such as large diameter pile shafts, where the laterally spreading soil flows around the pile and the ultimate soil reactions mobilize. In those cases, the soil reactions, and therefore the bending moments, are not necessarily dependent on the soil displacements in which case imposing the permanent (end of shaking) soil displacements may be adequate in design.
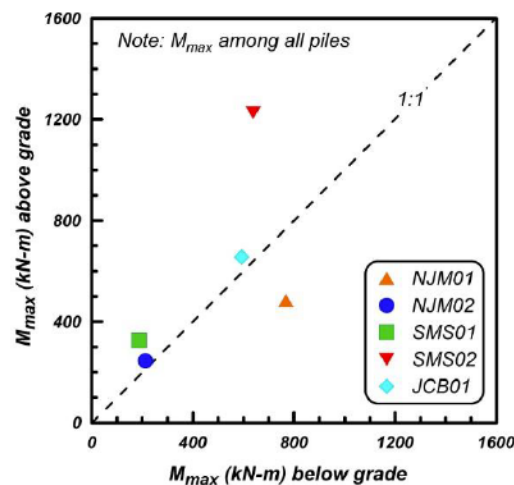

Figure 4. Comparison of the maximum bending moments above and below grade

IMPLICATIONS OF THE PHYSICAL MODELING FOR COMBINING INERTIAL AND KINEMATIC DEMANDS

The physical model tests provided a very worthwhile data set that highlights the depth-, pile row-, and time-dependent interaction of inertial and kinematic effects leading to the cumulative loads on piles for five different prototypes of wharf and waterfront configurations. The data clearly demonstrates that the moments resisted along a single pile reflect a complex interaction of ground motion characteristics, wharf – pile stiffness and dynamic response, and the combination of transient and accumulated permanent ground deformation. As addressed in ASCE 61-14, it is therefore necessary to approximate the primary lateral loads (inertia and kinematics) acting on a single pile and combine these loads in a manner that satisfies performance objectives for all piles supporting the wharf throughout the entirety of the design seismic load application (i.e. duration of shaking).

The use of inertial and kinematic Load Combinations is commonly applied in practice as

addressed in the Introduction; however, a broad range of scaling factors to peak loads have been proposed. To investigate whether inertial demands applied at the pile head should be combined with kinematic demands to estimate large bending moments at various locations along a pile pseudo-static analyses of the five centrifuge models addressed herein were performed with *LPILE*. Each of the five models were analyzed for two earthquake load sequences, thus 10 earthquake loading scenarios were evaluated. The bending moments computed using *LPILE* were compared against the measured moments from the centrifuge tests. The profiles of moment along the pile were compared; however, for the sake of brevity the results presented in this paper focus on the portion of the piles where large bending moments were observed during the centrifuge tests. This comparison provided a practical approach to determine whether inertial and kinematic demands should be combined in order to estimate bending moments at different depths. The following three load combinations were evaluated:

- Kinematic demand only: Soil displacement profiles were extracted at the time of maximum bending moments at depth from centrifuge tests and were applied to the end nodes of p-y springs. The soil displacement profiles were calculated by combining the transient component (from accelerometers) and the permanent component (from LVDT at ground surface).
- Wharf inertial demand only: Inertial forces at the pile head were extracted at the time of the maximum bending moment at depth in the centrifuge tests, and were applied to the pile head as shear forces. The inertial force was calculated from the slope of the bending moment profiles above the grade for the piles that were instrumented. The pile-deck connection was modeled as fixed-head given the non-yielding connection and the in-plane rigidity of the wharf deck.
- Combined kinematic and inertial demands.

It is important to note that these demands (i.e. the inertial load applied at pile head and soil displacements imposed along the piles) are often estimated in practice on the basis of decoupled analyses. In this study, these demands were not estimated; they were directly extracted from the centrifuge tests. In the absence of strong motion records at design-level seismic loads on well-instrumented wharves in North America, the physical modeling results provide useful data for evaluating how inertial and kinematic loads from decoupled analyses (i.e., *LPILE*) should be combined to yield a representative approximation of the measured, coupled behavior of wharf – pile – soil interaction. The goal of this on-going investigation is to develop rational procedures for combining the individual loads for a practice based analysis.

The comparison of bending moments at the pile heads obtained from *LPILE* and the corresponding centrifuge tests is provided in Figure 6a. The trends from the 10 tests evaluated demonstrate the following general conclusions;

- Applying combined inertial and kinematic demands provides the best agreement between the *LPILE* simulation and the physical modeling results,
- Applying inertial demands only will slightly underestimate the bending moments,
- Applying kinematic demand only will grossly underestimate the bending moments, as expected.

Although it is anticipated that the bending moments at pile heads are primarily driven by the inertial forces due to the wharf deck, as evidenced by the majority of data points that are reasonably estimated by applying inertial demands only, the data trends support combining inertial and kinematic demands to capture the response.

The comparison of the bending moments from physical and numerical models for deep

locations (>10D) associated with deep-seated ground deformation is provided in Figure 6b. As anticipated, the effects of the inertial loads decreases with depth. The data trends support the application of kinematic loading only as the combination of inertial and kinematic demands did not improve the accuracy of estimated bending moments at depth.
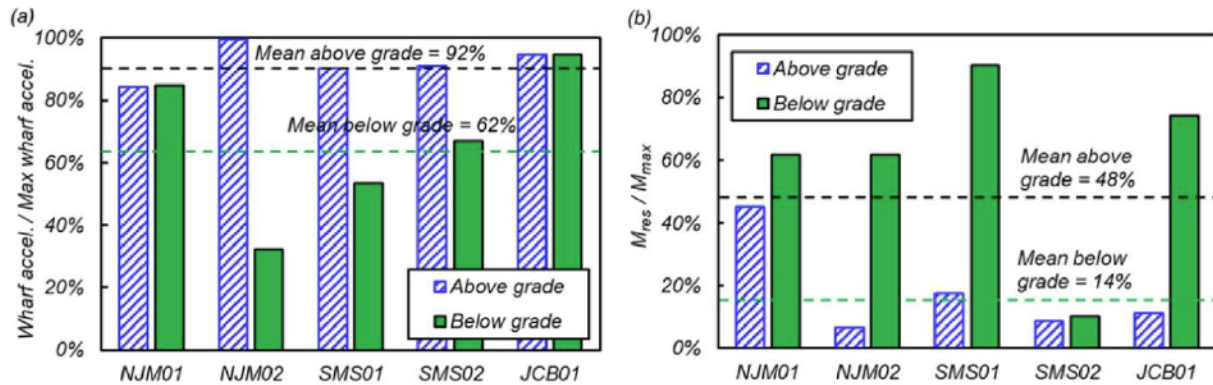

Figure 5. (a) Normailized wharf accelerations at the time of maximum bending moments, and (b) ratios of residual bending moment to maximum transient moments above and below grade
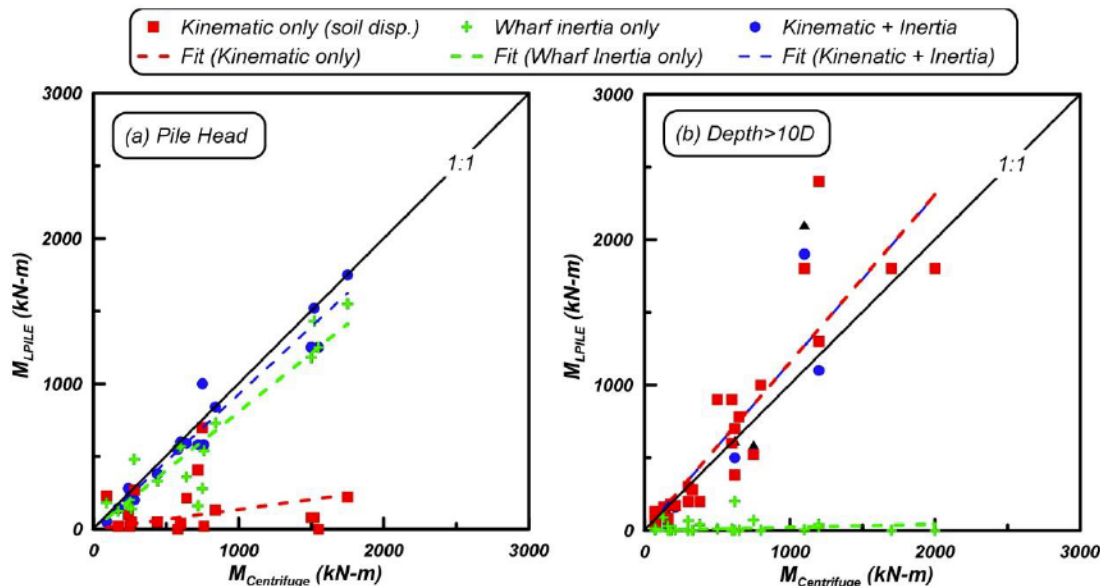

Figure 6. Comparison of bending moments recorded in the centrifuge tests and estimated from *LPILE* models

CONCLUDING REMARKS

Physical modeling of the dynamic response of five well-instrumented wharf – foundation configurations has provided an extensive database for evaluating complex soil-foundation-structure interaction and for calibrating numerical models routinely used in practice for wharf design. This paper has focused on a subset of the instrumentation array data that supports the investigation of dynamic loading of the wharf foundation piles. The primary results of the investigation are summarized as follows, with suggestions for the seismic analysis of pile supported wharves in practice.

1. Practice-oriented procedures for combining Inertial and Kinematic loads on piles are considered necessary approximations of complex soil-foundation-structure-interaction (SFSI) that has been shown by the physical modeling to be dependent on factors such as; pile row, location along the pile, wharf – foundation stiffness, soil profile and site configuration, and ground motion characteristics. This complexity has led to the development of Load Combination factors that are derived from envelops of maximum response along a pile, therefore do not explicitly account for the timing of the respective loads. The results of the physical modeling and subsequent pseudo-static analyses support the following practical approximations for seismic wharf design;
   a. Peak bending moments adjacent to the pile head (roughly in the upper 3D to 6D) approximated using only peak wharf deck inertial loads (100% I + 0% K) provide estimates that generally fall within 0.70 to 0.85 x Peak Measured Moment; however, substantially smaller ratios were observed. Peak moment estimates at the pile head were improved by incorporating the effects of kinematic loading, which largely accrues due to rotation at the pile-deck connection in response to global ground displacement.
   b. In general, peak pile moments at depth (> 10D) can be reasonably evaluated using the displacement demand (i.e., soil displacement profile) without the contribution of inertial loading, thus 100% K + 0% I.

2. Although in all five tests studied here the inertial load and soil displacements were in-phase (in bayward or landward directions) at the time of maximum bending moments, the soil reaction along the nonliquefiable crust (i.e. rockfill) was not necessarily in-phase with the wharf inertia. For relatively flexible piles, such as those studied here, the piles closely follow the soil deformations. As a result, the sign of the lateral soil reaction changes through the rockfill and non-liquefiable, near-surface soils. Therefore, it is overly conservative to assume that the near-surface soils apply a uniformly bayward pressure on the piles. In these cases, the kinematic demands can be best estimated by imposing the soil displacements to the end nodes of p-y springs, rather than imposing them as a lateral spreading pressure. Applying kinematic demands using a uniformly bayward passive pressure from the rockfill in pseudo-static analysis significantly overestimated bending moments in piles.

3. In almost all tests (except SMS02 where kinematic demands were minimal) large bending moments developed at depths greater than 10D, which is below the typically assumed equivalent depth of fixity.

4. Transient, peak moments at both the pile head and at depth are often greater than the end of shaking residual moments. This is attributed to the difference between the maximum transient and permanent (end of shaking) soil displacements. The data from the five centrifuge tests suggest that the maximum transient soil displacements were 1.3 to 2.7 times larger than the permanent soil displacements. When existing design methods are used to estimate soil displacements, the uncertainties in the estimated values should be considered in design. If the results of 2D nonlinear dynamic analysis are used by the designer in supplementary pseudo- static (uncoupled) analysis, the computed peak transient displacement should be considered as opposed to the end of shaking residual ground displacement. If the Newmark sliding block analysis is used to estimate soil displacements, the built-in conservatism in computing the accumulated permanent displacement should be considered in design. There is also considerable uncertainty in

estimating the soil displacement distribution with depth which was found to significantly affect the estimated bending moments in *LPILE* analyses for the flexible piles that were studied here. Additional work is needed to assess the accuracy of existing design methods in estimating maximum transient soil displacements and their distribution with depth in layered and challenging soil profiles. This should be noted in dynamic geotechnical analyses in which peak kinematic loads are often evaluated using the end of shaking, residual soil displacement profile.

5. It is important to note that this investigation did not include important aspects of pile response and performance due to loads associated with dynamic p-Δ effects for piles supporting crane rails and therefore additional vertical loading imposed by gantry cranes.

ACKNOWLEDGMENTS

REFERENCES

AASHTO (2014). "Guide Specifications for LRFD Seismic Bridge Design." Second Edition with 2014 Interim, AASHTO, Washington, D.C.

ASCE/COPRI 61-14 (2014). "Seismic Design of Piers and Wharves, prepared by the ASCE Standards Comm. on Seismic Design of Piers and Wharves." ASCE, Reston, VA.

Brandenberg, S. J., Boulanger, R. W., Kutter, B. L., and Chang, D. (2005). "Behavior of pile foundations in laterally spreading ground during centrifuge tests." Journal of Geotechnical and Geoenvironmental Engineering, ASCE, 131(11), 1378-1391.

California Department of Transportation (Caltrans) (2012). "Guidelines for Foundation Loading and Deformation Due to Liquefaction Induced Lateral Spreading." Sacramento, CA.

Chou, J. C., Kutter, B. L., Travasarou, T., & Chacko, J. M. (2011). "Centrifuge modeling of seismically induced uplift for the BART Transbay Tube." Journal of Geotechnical and Geoenvironmental Engineering, 137(8), 754-765.

Dobry, R., Abdoun, T., O'Rourke, T.D., and Goh, S.H. (2003). "Single piles in lateral spreads: Field bending moment evaluation", J. Geotech. Geoenviron. Eng. 129, 10, 879-889.

McCullough, N. J., Dickenson, S. E., & Schlechter, S. M. (2001). "The seismic performance of piles in waterfront applications." In Ports' 01: America's Ports: Gateway to the Global Economy (pp. 1-10).

Oregon Dept. of Transportation (2014). Geotechnical design manual. Tech. Services Branch, Salem, OR.

Travasarou, T., Chen, W. Y., & Chacko, J. M. (2011). "Liquefaction-induced uplift of buried structures: insights from the study of an immersed railway tunnel." In Proc. of 5th International Conference on Earthquake Geotechnical Engineering, Chile, January.

Washington Department of Transportation (WSDOT) (2015). "Geotechnical Design Manual." M 46-03.11, May 2015.

Zhou, Y. G., Chen, J., Chen, Y. M., Kutter, B. L., Zheng, B. L., Wilson, D. W., and Clukey, E. C. (2017). "Centrifuge modeling and numerical analysis on seismic site response of deep offshore clay deposits." Engineering Geology, 227, 54-68.